

5012.2  
Düren/1  
~~copy~~

*Lehrstuhl für Flugzeugbau*

TECHNICAL MEMORANDUMS  
NATIONAL ADVISORY COMMITTEE FOR AERONAUTICS

-----  
No. 756  
-----

THE BEHAVIOR UNDER SHEARING STRESS OF DURALUMIN STRIP  
WITH ROUND, FLANGED HOLES  
" "  
By Karl Schussler

Luftfahrtforschung  
Vol. 11, No. 3, August 19, 1934  
Verlag von R. Oldenbourg, München und Berlin

4.3.12  
4.7.5  
Washington  
October 1934

NATIONAL ADVISORY COMMITTEE FOR AERONAUTICS

TECHNICAL MEMORANDUM NO. 756

THE BEHAVIOR UNDER SHEARING STRESS OF DURALUMIN STRIP  
WITH ROUND, FLANGED HOLES\*

By Karl Schüssler

SUMMARY

This report presents the results of an investigation to determine the behavior of duralumin strip with flanged holes in the center when subjected to shear stresses. They buckle under a certain load just as a flat sheet. There is one optimum hole spacing  $a_0$  (equation 4) and one corresponding buckling load in shear  $p_{k0}$  (equation 7) for each sheet width, sheet thickness, and flange form. Comparison with nonflanged sheets revealed a marked increase of buckling load in shear due to the flanging and a slightly greater displacement. The stiffening effect of flanging showed itself in a considerably higher buckling load for thin, wide strip than for the unweakened sheet. Lastly, the displacement  $\delta$ , under a 1 kg/mm (55.99 lb./in.) load (equation 8) was determined. It is considerably higher for the flanged sheet than for the unweakened sheet, and slightly higher than for the unflanged sheet. Sheets may not be stressed beyond buckling load unless special cross stiffeners are available to take up the load component  $K$  perpendicular to the direction of shear. The shear-displacement diagram (fig. 6) is substantially a tensile stress-strain diagram above the buckling load. The formulas developed for  $a_0$ ,  $p_{k0}$ , and  $\delta$  are the results of pure experimentation and may therefore become quite faulty outside of the analyzed range.

---

\*"Über das Verhalten von Leichtmetallblechstreifen mit kreisrunden, randgebördelten Lochern bei Schubbeanspruchung." Luftfahrtforschung, August 18, 1934, pp. 74-85.

.INTRODUCTION.

A very popular structural member in light-metal airplane and airship design is the flat, thin metal strip with lightening holes, the edges of which are generally flanged for reasons of stiffness.

The loads are, as a rule, not taken up by the individual sheet since it forms, with other sheets, corrugated sheets, rods, or angles, an elastic structure: such as of a spar, compound spar of two or more spars, float frame, airship girder, etc.

The location of the forces relative to the elastic axis of the system is essential for the type of stress. The forces lying on a plane with this axis simply set up tension, compression, or bending in the elastic structure, whereas all others effect an additive torsion. This stresses, apart from specific cases, the individual sheets in shear. When the forces are at great distance from the elastic axis, the shear may become so great as to make the other stresses negligible; that is, make it a case of simple shearing stress.

NOTATION

a mm, hole spacing.  
a<sub>0</sub> " optimum hole spacing.  
b " width of sheet.  
d " diameter of hole.  
D " diameter of flanging.  
E kg/mm<sup>2</sup>, Young's modulus.  
G kg/mm<sup>2</sup>, modulus of shear.  
L mm length of sheet.  
P kg/mm, shearing stress.  
P<sub>k</sub> " buckling load in shear.

---

(kg/mm<sup>2</sup> × 1422.35 = lb./sq.in.) (mm × 0.03937 = in.)

- $p_{k0}$  kg/mm,  $p_k$  value of  $a_0$ .
- $p_{ku}$  "  $p_k$  value for smooth sheet.
- $P$  kg, shearing force.
- $r$  mm, distance of last hole from edge.
- $s$  " thickness of sheet.
- $v$  " displacement.
- $v_k$  " displacement during buckling.
- $\delta$   $\frac{\text{mm}}{\text{kg}}$ , displacement for  $P = 1$  kg (2.20462 lb.).
- $\delta_1$  mm  $\frac{\text{mm}}{\text{kg}}$ , relative displacement for  $p = 1$  kg/mm.
- $\mu$ ,  $10^{-3}$  mm.

#### PREVIOUS SHEAR INVESTIGATIONS ON METAL STRIP

The behavior of infinitely long, flat strip in shear is determined by calculation and the calculation is checked by experiment. The sheet remains flat at first and the displacement  $v$  is proportional to the shear load  $p$ :

$$v = \frac{p b}{G s}$$

where  $b$  = width,  $s$  = gage of sheet, and  $G$  = shear modulus of the structural material.

Upon reaching a certain shear load uniform corrugations or waves are formed which at first run at about  $45^\circ$  in the direction of shear, and  $v$ , rather than remaining proportional to  $p$ , now increases; the sheet buckles (fig. 1).

Bryan, Lilly, Timoschenko, and Ritz (references 1 to 5) have developed approximations for computing the buckling stress in shear and the spacing of the wrinkles  $\lambda$ , while Southwell and Skan (reference 6) found the rigorous mathematical solution. As with the compression member, it results in an infinite series of load values at which the

flat sheet stressed in shear is unstable; that is, buckles. The lowest and therefore decisive value is:

$$P_{ku} = \frac{88.7 E s^3}{12 \left[ 1 - \left( \frac{1}{m} \right)^2 \right] b^2} \quad (2)$$

where  $E$  = Young's modulus and  $m$  = Poisson's ratio of the material. The corresponding wave length is:

$$\lambda = 1.6 b \quad (2a)$$

These mathematical results were checked against buckling in shear experiments. With shear distributed uniformly along whole sheet length  $L$ , the shear force  $P$  and  $L$  give  $p = \frac{P}{L}$  or, if two identical sheets are stressed concurrently,

$$p = \frac{P}{2L} \quad (3a)$$

But with finite sheet length  $p$  must drop to zero at the free ends; that is, it cannot be constant across  $L$ . The last elements at the free ends cannot transmit the shear forces to adjacent elements; i.e., they must be shear free.

According to Coker's experiments below the buckling limit (reference 7), sheets which are very long in comparison with their width manifest a shear load  $p$ , which is practically constant across the whole length and only drop on a short piece at the edge. In approximation we may assume  $p = 0$  on two end strips of length  $b/4$  and constant on the intermediate piece of length  $L - 2 \frac{b}{4} =$

$L - 0.5 b$ . This gives  $p = \frac{P}{L - 0.5 b}$ , or for two identical sheets:

$$p = \frac{P}{2L - b} \quad (3b)$$

The buckling tests in shear made by Bollenrath (reference 8) gave a buckling load in shear of about 43 percent according to (3a), and of about 37 percent, according to (3b) below the theoretical value computed according to (2). Even the wave length varied from the theoretical value  $\lambda = 1.6 b$  (2a), averaging 1.94  $b$ .

Mathar (reference 9) explained these discrepancies as follows: The shear force is not evenly distributed over the whole length of the clamping strips, but introduced only at one or two places. The elastic strips must take up the shear forces and become elongated. The displacement and through it the shear load  $p$  is, as a result, higher at the points contiguous to the applied load than farther away. On the other hand, buckling is contingent upon the maximum value of  $p$ , because as soon as  $p$  exceeds  $p_{ku}$  (equation 2) at any place, buckling must occur. Owing to favorable, i.e., relatively rigid fixation, Mathar obtained buckling figures which are only 5 percent below  $p_{ku}$ , and a wave spacing of 1.6  $b$ , that is, corresponding to the theoretical figure (equation 2a).

Seydel (reference 10) analyzed flat, rectangular plates with stiffeners parallel to the edges and adduced an example of transversely riveted angle stiffeners.

Schmieden (reference 11) computed very thin, infinitely long sheets with superposed, closely spaced small cross stiffeners, to which longitudinal stiffeners may be added. The mathematical accuracy of his formulas is dependent upon all very small quantities becoming infinitely small.

Bergmann and Reissner (reference 12) approximated corrugated sheets with corrugations parallel or perpendicular to the direction of shear as flat plates with varying bending stiffness in the two mutually perpendicular directions.

Jennissen (reference 13) experimented on corrugated plates divided by brackets in separate panels. He developed an approximative method for their calculation and obtained a close agreement between experiment and theory. The problem of sheets weakened by holes has equally been attacked.

Hirota (reference 14) calculated the stress attitude prior to buckling in an infinitely long metal strip with a hole in the center when stressed in shear.

Mathar (reference 9) determined experimentally the buckling load of strip with round holes evenly spaced over the center line. He found that holes of  $d = 70$  spaced  $a = 140$  mm, reduced the buckling load in a duralumin strip ( $s = 0.7$  mm,  $b = 110$  mm) by about 50 percent while raising  $v$  by nearly 110 percent.

The present experiments were primarily intended to ascertain whether it would be possible to stiffen a sheet weakened by holes with flanging the holes' edges enough to assure a buckling load  $P_k$  approaching or even exceeding the buckling value of the unweakened strip  $P_{ku}$  (equation 2).

#### EXPERIMENTAL SET-UP

The experimental arrangement is that developed from Mathar's and Jennissen's tests. It is shown in figure 2.

Two identical strips are clamped between two stationary end rails and one sliding center rail at which the shear is applied. Naturally the fixed spacing of the side rails produces minor additive tension perpendicular to the direction of shear with the displacement which, however, may be disregarded with respect to the shearing stresses; with  $\alpha$  = angle of displacement the width  $b$  should diminish to  $b \cos \alpha$ . As  $\alpha$  remained consistently below  $0^\circ 20'$  up to buckling, the additive tensile stress could at the most reach  $(1 - \cos 0^\circ 20')$   $E$ ; that is,  $(1 - 0.99997) \times 7,500 = 0.235 \text{ kg/mm}^2$ , while in general it amounted to only a fraction of this figure because  $\alpha$  is mostly considerably lower.

The force was measured with a tension stirrup up to 20 t (point 1, fig. 2) and a compression dynamometer up to 10 t for high loads in isolated tests (point 2, fig. 2). The possible error for the tensiometer was  $\pm 8 \text{ kg}$ . As  $P_k$ , the buckling load in shear, is  $\geq 500 \text{ kg}$  in all tests, this error amounts to  $\leq \frac{8}{500}$ , that is  $\leq 1.6$  percent.

With compression gage added, the possible error is  $\pm 7 \text{ kg}$  higher for instrument friction and error in reading as well as  $+19 \text{ kg}$  for each  $1^\circ \text{ C.}$  temperature rise caused by the expansion of the mercury in the dynamometer. Without temperature correction this error is below  $\pm 38 \text{ kg}$  corresponding to  $2^\circ \text{ C.}$ , with correction  $\pm 9.5 \text{ kg}$  or equivalent to  $0.5^\circ \text{ C.}$  temperature error in the pressure recorder. The total instrumental error is therefore  $7 + 38 = 45 \text{ kg}$  in the first, and  $7 + 9.5 = 16.5 \text{ kg}$  in the second case. The total error in shear is under the most adverse conditions,  $8 + 45 = 53 \text{ kg}$  without, and  $8 + 16.5 = 24.5 \text{ kg}$  with temperature correction. Compared to only  $8 \text{ kg}$  without compression gage, these errors are high, for which reason the measurements were as a whole made only with the tensiometer.

(t (ton)  $\times 2204.62 = \text{lb.}$ )

The displacement was recorded with the Zeiss dial gage (point 3, fig. 2). As a check, we used the Martens mirror instrument in some tests (points 4a and 4b in fig. 2). The dial gage admits of an error in reading of 0.001 mm. The displacement at the point of collapse  $v_k$  was always  $\geq 0.074$  mm, so the percentage of error was always  $\cong \frac{0.001}{0.074} = 1.4$  percent.

The error due to elongation of the center rail which transmits the shearing force is also small. Working with the tensiometer alone (most unfavorable case) and assuming  $p$  to be constant over the whole length  $L$ , the force to be transmitted by the center rail from the beginning to the end of the strip drops linearly from  $P$  to zero; it averages  $0.5 P$ . The corresponding mean stress is  $\sigma_m = \frac{0.5 P}{F} = \frac{0.5 P}{2 B H}$ , where  $B$  and  $H$  represent the width and height of the upper and lower half of the center rail. Owing to this stress the rails have a total elongation of  $\delta = \frac{\sigma_m L}{E} = \frac{0.5 P L}{2 B H E}$ . With a displacement  $v$  for a perturbation  $P$ , the relative discrepancy in displacement and consequently that of its proportional shear load  $p$  amounts at the most to:

$$\frac{\delta}{v} = \frac{0.5 P L}{2 B H E v} = \frac{0.5 L P}{2 B H E v}$$

$\frac{P}{v}$  is maximum for strip 33:  $P_k = 3,000$  kg;  $v_k = 0.162$  mm. Therefore,

$$\frac{\delta}{v} = \frac{0.5 \times 1192}{2 \times 160 \times 32 \times 21000} \times \frac{3000}{0.162} = 0.051 = 5.1 \text{ percent.}$$

This discrepancy between maximum and minimum  $p$  corresponds to a difference of about  $\pm 3$  percent from the mean value.

In the most unfavorable case the total error equals the sum of the individual quotas:

$$f_{\text{total}} \cong 1.6 + 1.4 + 3 = 6 \text{ percent.}$$

The buckling was also determined separately from the wrinkles which caused the image of a cross in the sheet to become distorted.



### GENERAL RESULT OF BUCKLING TESTS

The samples were duralumin 681b of the Düren Metallwerke, in strips of 2500 X 500 mm length and of 0.4, 0.5, 0.6, and 0.8 mm thickness. Its Young's modulus was  $E = 7,500 \text{ kg/mm}^2$ , with a shear modulus of  $G = 2,900 \text{ kg/mm}^2$ .

Aside from several flat strips and one perforated strip without flanging, the rest all had flanged holes - each pair of strips having the same hole diameter, spacing, and type of flanging.

The flanging was beveled. The form is shown in figures 3 and 4 along with the male and female dies. The bevel angle was made the same as the friction angle with grease lubrication to allow smooth removal of the male die after flanging operation.

The preparation of the samples was effected with great care. They were cut out to the correct length and width and, if necessary straightened. The holes were drilled to  $1/10$  diameter (centering hole) and then cut out with a cutting tool. The flanging operation consisted of pushing with male and female dies (fig. 4).

We investigated the effect of:

1. Strip width,  $b$ .
2. Strip thickness,  $s$ .
3. Diameter of flanging,  $D$ .
4. Depth of flanging. This may be changed for given flanging form by means of the cut-out hole diameter,  $d$ : flanging depth  $\approx 0.5 (D - d)$ .
5. Hole distance,  $a$ .

The flanged strip behaved the same as the flat strip under shearing stress. Up to a certain load stage, the strip remained flat, the shearing force  $P$  is proportional to the displacement  $v$ . The distance of the wrinkles equals the hole spacing  $a$ . The test points deviate simultaneously from the previous straight line and follow a new straight line after a few points (fig. 6). The center of the two straights was taken as the buckling point of

the strip. With further stress the curve deviates from the straight line because the yield point is soon exceeded as a result of the great deformation of the buckled strip. Figure 7 shows a curve with several unloadings. This graph is valid only for constant strip width  $b$  under load as in the present experiments. The shearing force  $S$  before buckling (fig. 8, left) assumed divided in tension  $Z$  and compression  $D$  consists, after the strip buckled with respect to compression  $D$  (fig. 8, right of  $D$  which, analogous to the buckled compression member, remains practically constant), of tension  $Z$  and a new component  $K$  perpendicular to the direction of shear.  $Z$  and  $K$  grow in the same proportions as  $S$ . In relation with  $Z$  and therefore  $S$  the extension of the visualized tension members and through them the displacement  $v$ , is proportional to the elongation due to  $Z$ . Figure 7 is therefore essentially a stress-strain diagram. The  $K$  component in the present experiments is taken up by the clamping rails. In practical cases, however, a stress above the buckling limit is possible only when there are special cross stiffeners to take up  $K$ . In simple strips the two longitudinal edges come consistently closer together because of  $K$ ; the strip is destroyed in the present experiments through tearing of the flanged edges. Figure 9 shows a severely deformed, torn strip. The deformation, considerably magnified, is the same as immediately after buckling (fig. 5).

The majority of tests was made with strip lengths of  $L \cong 1,192$  mm. The buckling force in shear of the flanged strip  $P_k$  should be assumed proportional to the strip length, as shown in figure 10. The buckling load in shear  $p_k$  is defined from the buckling force in shear  $P_k$  and strip length  $L$  according to (3a):

$$p_k = \frac{P_k}{2L} \quad (3)$$

The figures in figure 10 are those of table I for strip 17 to 19, 41 to 45, and 47. The displacement in buckling  $v_k$  (in mm) is for identical sheets of varying length, naturally always the same, because the sheet consists of identical strips of length  $a$  which, regardless of their number, are identically distorted.

The effect of the flange depth is subordinate as seen from table I, sheets Nos. 43 to 45.  $P_k$  remains constant within wide limits with increasing  $d$ , that is, decreas-

ing flange depth  $0.5 (D - d)$ , while  $v_k$  shows a slight increase for smaller flange depth. The explanation for this behavior is that for deflection perpendicular to the plane of the sheet, that is, for buckling, the flanged hole should be considered as rigid relative to the sheet, as soon as the flanging has reached a certain minimum depth. By the same argument, not the flanged hole but rather the part of the sheet which remained flat, is the decisive factor for the buckling load since it remains the same in any case when  $d$  is changed. On the other hand, the flanging is more readily bent in the direction of the plane of the sheet than the unweakened, flat part of the sheet. Consequently, a deeper - that is, stronger - flanging assures less displacement for identical load.  $P_k$  is essentially more important for the designer than  $v_k$ . But any improvement in the flanging can only involve an improvement of  $v_k$ , not of  $P_k$ , because  $P_k$  is governed by the flat part of the sheet. In general, the form of flanging is therefore subordinate when it has a certain minimum stiffness perpendicular to the plane of the sheet only with given  $D$ . Logically,  $D$  only needed to be changed, but not  $d$ .

The flanging operation increases the perimeter of the hole from  $\pi d$  to  $\pi D$ , and it is necessary to assure that the resulting unit elongation  $\frac{\pi (D - d)}{\pi d} = \left(\frac{D}{d} - 1\right)$  does not exceed the ultimate, because the edges would tear otherwise. Small irregularities on the edge of the hole act as notches very favorable for tearing. With smoothly cut holes flange tearing can be safely avoided in the kind of material and the shape of flanging used here when  $d \geq 0.85 D$ .

Figure 11 shows the effect of hole spacing  $a$  versus buckling load  $P_k$ . The curves have a distinct maximum for comparatively small  $a$ , which lies above or below the shear load in buckling of the unweakened sheet  $P_{ku} = P_{ku} (2L - b)$ . (Compare equations (2) and (3b).) The maximum is due to the fact that the flanging as already pointed out is rigid in bending perpendicular to the plane of the sheet as compared to the unweakened sheet, while being more easily deformable in direction of the plane of the sheet than the unweakened sheet; i.e., takes up practically no shearing stress. The greater the number of flanged holes in a sheet, the greater is the number of bending resistant circular surfaces of diameter  $D$ ; the higher is

the value at which the sheet wrinkles perpendicular to its plane. On the other hand, the sheet which, after all, is supporting only in the flat portion, is so much higher stressed as there are holes. Both effects are contrariwise, hence the maximum.

The behavior with wide-hole spacing  $a$  was not investigated. With very high  $a$  values, that is, few holes, the  $p_k$  value should approach the buckling value of the flat sheet without holes  $p_{ku}$  (equation 2). Other extreme values may appear between these limits, but they are not very important because the holes must, for reasons of weight saving, be spaced as closely as possible. In the following, no importance therefore was attached to the maximum other than for small  $a$ . All values valid for this maximum carry the subscript  $o$ .

#### OPTIMUM HOLE SPACING $a_o$

The first significant question is, the best hole spacing  $a_o$  at which the maximum occurs for a given sheet thickness  $s$ , width  $b$ , and diameter  $D$ . It is not necessary to define  $a_o$  very accurately because the contiguous  $P_k$  values do not vary appreciably from  $P_{ko}$  maximum when  $a$  deviates a little from  $a_o$ , owing to the horizontal tangent of the curves  $P_k = f(a)$ .

The effect of  $b$  on  $a_o$  was so little in the analyzed range as to escape definition. The reason for this is that the center strip of the sheet governs the buckling. But this strip naturally has always the same aspect for otherwise identical sheets of different width.

The relationship between  $a_o$  and  $s$  is parabolic, according to table II and figure 12:  $a_o = \alpha s$ ;  $a_o$  increases considerably with increasing  $s$  for thin sheets, less for thicker sheet. The reason for this is that the bending stiffness of the sheet rises perpendicularly to its plane with  $s$ , while the stiffness of the flanging increases only with  $s$ . Admittedly, the stiffening effect of the flanging is not as great for thicker sheets which of themselves are already very stiff, so that the holes must be spaced farther apart than in thinner sheets. The explanation for the smaller rise of the curve of thicker

sheets is that, for example, a 0.1 mm thickness change means comparatively less in a thick than in a thin sheet.

The factor  $\alpha$  varies in linear relation with  $D$  (table II and fig. 13):  $\alpha = 68.5 + 0.8 D$ . Consequently,

$$a_0 = \alpha \sqrt{s} = (68.5 + 0.8 D) \sqrt{s}$$

$$a_0 = 0.8 (D + 86) \sqrt{s} \quad (4)$$

Far outside of the investigated range:  $D = 62$  to  $82$ ,  $s = 0.4$  to  $0.8$  mm,  $b = 75$  to  $215$  mm, the strictly experimental equation (4) may become quite defective. Furthermore, it is valid only so long as the flanging does not touch the sheet border

$$D < b \quad (5a)$$

and the flanging does not overlap:

$$D < a_0 = 0.8 (D + 86) \sqrt{s}.$$

whence

$$D < \frac{86 \sqrt{s}}{1.25 - \sqrt{s}} \quad (5b)$$

The last equation (5b) expresses the selection of  $D$ , especially for thin sheet. If it is not complied with the best value for the buckling load in shear  $P_{k0}$  is not within the constructively possible range; the holes would be greater than the spacing; the flangings would run into each other. For the thinnest sheet examined,  $s = 0.4$  mm,

it is necessary that  $D < \frac{86 \sqrt{0.4}}{1.25 - \sqrt{0.4}}$  or  $D < 88.5$  mm

according to equation (5b), while the diameter of the greatest flanges was only  $D = 82$ .

TABLE II

D mm	s mm	a <sub>0</sub> mm	$\sqrt{s}$	$a = \frac{a_0}{\sqrt{s}}$	
62	0.42	76	0.648	117.5	α = 118
	.52	85	.721	118	
	.615	93	.784	118.5	
	.8	100?	.894	112?	
72	0.52	90	0.721	125	α = 125
	.8	> 89	.894	> 99.5	
82	0.42	89	0.648	137.5	α = 135
	.52	97	.721	134.5	
	.615	{100 110.5	.784	{127.5 141	
	.8	> 106.5	.894	> 119	

BUCKLING LOAD IN SHEAR  $P_{k0}$  AND ITS PERTINENT  $a_0$

When stressing sheets of the examined kind in shear the best hole spacing  $a_0$  (equation 4) must be adhered to if at all possible, to assure high loading without buckling. With this in mind, we did not determine  $P_{k0}$  for any hole spacing  $a$ , but rather the optimum  $P_{k0}$  for each pair of sheets of  $L = 1.192$  mm with optimum hole spacing  $a = a_0$ .

For equal  $b = 110$  mm and equal  $D = 62$ ,  $D = 72$ , and  $D = 82$ , the  $P_{k0} = f(s)$  values lie on three straight lines which intersect in a point with the coordinate  $s = 0.54$  mm  $P_{k0} = 1,700$  kg (fig. 14). This intersection point shall be the common point of all  $P_{k0} = f(s)$  curves for  $D = \text{constant}$  and  $b = 110$  mm. For  $s = 0.54$  mm the size of  $D$  is accordingly immaterial. In all

sheets of 0.54 mm thickness.  $P_{ko}$  is the same, provided  $a = a_0$ . For

$$s < 0.54 \text{ mm, } D \text{ must be small,} \quad (6a)$$

$$s > 0.54 \text{ mm, } D \text{ must be great.} \quad (6b)$$

For thicker, inherently stiff sheets, the flangings must be equally stiff; that is, be of a certain depth which, in turn, is contingent upon large diameters.

The straight lines through the point [ $s = 0.54$  mm,  $P_{ko} = 1,700$  kg] may be expressed with

$$P_{ko} = 1700 + \beta (s - 0.54),$$

wherein  $\beta$  depends on  $D$ . According to figure 15, it is proportional to  $D$ . With  $\beta = 95.6 D$ , the optimum  $P_{ko}$  for sheet of  $b = 110$  mm is:

$$P_{ko} = 1700 + 95.6 D (s - 0.54).$$

The effect of  $b$  on  $P_{ko}$  was not thoroughly explored because a few cursory tests proved it to be quite subordinate while on the other hand, an exact elucidation of the effect of  $b$  would have entailed a very great number of further experiments. The small effect of  $b$  is due to the fact that the middle strip, weakened by holes, is above all decisive for the buckling, while the flat-edge strips are but little effective. It is therefore justified to assume that for sheets of different width the behavior relative to the individual quantities is substantially the same.

To allow for  $b$  the values obtained for  $b = 110$  mm were given a correction factor dependent only on  $b$  and  $= 1$  for  $b = 110$  mm, while

for  $b < 110$  mm, it must be  $> 1$ ,

"  $b > 110$  " " " "  $< 1$ ,

because a narrow sheet does not buckle as easily as a wide one (equation 2). The correction factor  $f$  is tabulated in table III and plotted in figure 16.

TABLE III

D mm	s mm	a <sub>0</sub> mm	P <sub>k0</sub>				
			b=70 mm	b=90 mm	b=110 mm	b=175 mm	b=215 mm
62	0.42	76	1260		1130		
	.52	85	1720	1600	1530		
	.615	92.5			2220	1500	
	.8	104			3040		
72	0.42	81.3			900		
	.52	90.7			1520		
	.8	111.5			3200		
					4000		
82	0.42	86.3			760		
	.52	96.5			1600	(1000)	1400
	.615	105				1700	1500
	.82	118.5			3720	(1700)	

It is seen that the obtained values may be closely approximated with a hyperbola of the form of

$$f = \alpha + \frac{\beta}{b}$$

To define  $\alpha$  and  $\beta$  this formula is written as

$$f b = \alpha b + \beta,$$

a linear equation for  $f b$  in terms of  $b$ . The straight line is also shown in figure 16. It gives:



$$\alpha = 0.767$$

$$\beta = 25.6$$

whence

$$f = \alpha + \frac{\beta}{b} = 0.767 + \frac{25.6}{b} = 25.6 \left( 0.03 + \frac{1}{b} \right)$$

As the value for any  $b$  is to be  $f$  times as high as the  $P_{ko}$  value for  $b = 110$  mm, we find for any width  $b$

$$P_{ko} = 25.6 \left( 0.03 + \frac{1}{b} \right) [1700 + 95.6 D (s - 0.54)]$$

This value applies to a pair of sheets of  $L = 1192$  mm. The buckling load in shear  $P_{ko}$  being, according to figure 12, proportional to  $L$ , it is for  $L = 1$  mm, according to (3c):

$$P_{ko} = \frac{P_{ko}}{2 L} = \frac{P_{ko}}{2 \times 1192} = \frac{P_{ko}}{2384}$$

This formula, written in the preceding equation, gives the optimum  $P_{ko}$  value:

$$P_{ko} = \frac{25.6 \times 95.6}{2384} \left( 0.03 + \frac{1}{b} \right) \left[ \frac{1700}{95.6} + D (s - 0.54) \right]$$

For sheet with Young's modulus  $E$  not abnormally at variance with  $E = 7,500$  kg/mm<sup>2</sup>, the obtained  $P_{ko}$  value for  $E = 7,500$  kg/mm<sup>2</sup> must be multiplied by the correction factor  $E/7500$ :

$$P_{ko} = \frac{E}{7500} \times 1.03 \left( 0.03 + \frac{1}{b} \right) [17.8 + D (s - 0.54)]$$

$$P_{ko} = 1.36 \times 10^{-4} E \left( 0.03 + \frac{1}{b} \right) [17.8 + D (s - 0.54)] \quad (7)$$

This is on the premise that the buckling load in shear  $P_{ko}$  given in (7) is reached in kg/mm sheet length; that (4) is complied with, or in other words, that the optimum hole spacing  $a = a_0$  has been chosen. As equation (4), so can (7) become very defective outside of the range investigated; i.e., outside of  $D = 62$  to  $82$ ,  $s = 0.4$  to  $0.8$  mm,  $b = 75$  to  $215$  mm, because the formula merely repre-

sents an approximation formula from the obtained experimental values.

To show the accord of the optimum values of (7) with the experimental results, we computed  $P_{k0} = 2 L P_k$  with (3c) and (7), and included it in table I, together with the pertinent  $a_0$  value.

Admittedly, in airplane design a simple sheet shall never be so highly stressed as still allowed according to (7). Buckling generally occurs under lower shear stresses for various reasons. One thing is certain, however, and that is that it would serve no useful purpose to determine  $P_k$  more accurately than in the present experiments, because actual buckling occurs quite frequently at loads which are from 20 to 40 percent lower than the theoretical  $P_k$  value.

#### RELATIVE DISPLACEMENT $\delta_L$

Lastly, we determine the displacement of the non-buckled sheet. The shearing force  $P$  and the displacement  $v$  give the displacement of the sheets per 1 kg of tension at  $\delta_L = v/P$ , or with the values at buckling,  $P_k$  and  $v_k$  (table I),  $\delta_L = v_k/P_k$ . For sheets of length  $L \cong 1192$  mm (standard length), the subscript  $L$  is omitted on  $\delta_L$ . For these, we have:

$$\delta = \frac{v_k}{P_k} \left[ \frac{\text{mm}}{\text{kg}} \right], \quad \text{and} \quad \delta = 10^6 \frac{v_k}{P_k} \left[ \frac{\mu}{t} \right].$$

The effect of flanging depth, which may be varied as known, by means of the hole diameter  $d$  (fig. 6), is subordinate. In a sheet having the dimensions:

$$\begin{array}{lll} L = 1,690 \text{ mm}, & b = 110 \text{ mm}, & s = 0.515 \text{ mm} \\ D = 72 \text{ " } & a = 90 \text{ " } & r = 80 \text{ " } \end{array}$$

(sheets 43 to 45),  $\delta_L$  ranged between 127 and 133 mm when  $d$  rose from 62.5 to 65.45 and the flanging depth  $\sim 0.5 (D - d)$  dropped from  $\sim 4.9$  to  $\sim 3.275$  mm.

The explanation for this minor effect is that the flanged hole compared to the full sheet is easily deformable in direction of the plane of the sheet. (Note the weakness of the flanged hole compared to the sheet, in fig. 9.) The displacement is almost exclusively governed by the flat portion of the sheet.

Since the displacement  $v$  of a smooth sheet is inversely proportional to the thickness  $s$ , namely,  $v = \frac{P \cdot b}{G \cdot L \cdot s}$  (equation 1),  $\delta$  also must be inversely proportional to  $s$  for smooth, full (unweakened) sheets. But according to the tests on sheets with flanged holes  $\delta$  was not inversely proportional to  $s$  but needed, in addition, an exponent  $\beta$ :

$$\delta = \frac{\alpha}{s^\beta}$$

Plotted in logarithmic coordinates (fig. 17), we have  $\beta = 1.2$  for each investigated  $b$ ,  $D$ , and  $a$ , with  $\alpha$ , of course, depending upon these three quantities. To determine  $\alpha$  we multiplied the obtained  $\delta$  values with  $s^\beta$ :

$$\alpha = \delta s^\beta = \delta s^{1.2}$$

For the determination of the influence of  $a$  on  $\alpha$ , the space between the flanging ( $a - D$ ) is of prime importance. The greater the effective inter-space, the less is the displacement. The supposedly inverse proportionality ( $a - D$ ) fails to materialize; on the contrary ( $a - D$ ) must be augmented by an exponent  $\gamma$ :

$$\alpha = \frac{\epsilon}{(a - D)^\gamma}$$

The logarithmic graph (fig. 18) gives  $\gamma = 0.75$ ;  $\epsilon$  is as yet dependent on  $b$  and  $D$ . It may be defined from

$$\epsilon = \alpha (a - D)^\gamma = \alpha (a - D)^{0.75}$$

According to figure 19,  $\epsilon$  rises linearly with  $b$ . With the intersection of the straight lines for  $D = 62$  and  $D = 82$ , and the coordinates  $b = 310$  mm and  $\epsilon = 1230$  as the common intersection point of all straight lines  $D =$  constant, the equations for  $\epsilon$  become

$$\epsilon = 1230 - \lambda (310 - b)$$

with only  $\lambda$  dependent on  $D$ .

The linear course of  $\epsilon = f(b)$  and thereby of  $\delta = f(b)$  is due to the fact that for identical load the middle strip on otherwise identical sheets of different widths suffers approximately the same deformation and that the two flat-edge strips are augmented by a displacement proportional to the width of these edge strips. Logically, the whole displacement then increases in linear relation with  $b$ .

From the slope  $\lambda$  of the straight line  $\epsilon$  in figure 19, we assume it to change linearly with respect to  $D$ . Then figure 20 gives  $\lambda = 8.35 - 0.081 D$ .

The insertion of the obtained values  $\alpha$ ,  $\beta$ ,  $\gamma$ ,  $\epsilon$ , and  $\lambda$  yields:

$$\delta = \frac{1230 - (310 - b)(8.35 - 0.081 D)}{(a - D)^{0.75} s^{1.2}}$$

Loading the sheets in 1 kg/mm of sheet length over  $2L = 2 \times 1192 = 2384$  mm instead of in 1 kg gives the relative displacement  $\delta_1$ , which is  $2L$  times as high as  $\delta$ .  $\delta_1 = 2L \delta = 2384 \delta$ , when  $\delta$  is measured in mm/kg, and

$$\delta_1 = 2384 \times 10^{-6} \delta$$

when  $\delta$  is measured in  $\frac{\mu}{t}$  and  $\delta_1$  in mm  $\frac{mm}{kg}$ . The final result then is:

$$\delta_1 = 2384 \times 10^{-6} \times 0.081 \times \frac{1230 - (310 - b) \left( \frac{8.35}{0.081} - D \right)}{a - D^{0.75} s^{1.2}}$$

$$\delta_1 = 1.89 \times 10^{-4} \times \frac{15200 - (310 - b)(103 - D)}{(a - D)^{0.75} s^{1.2}} \quad (8)$$

To prove the agreement between the values obtained from (8) and the experimental data, table I shows the obtained  $\delta_1$  values together with the computed value. Equation (8) is based upon strictly experimental findings, hence its validity is assured for only the range investigated.

**COMPARISON WITH FULL SHEETS (NO HOLES) AND  
 SHEETS WITH HOLES BUT NO FLANGING**

In order to determine the suitability of flanged or plain holes as well as any eventual benefit accruing from such flanging, we investigated a sheet with and without flanged holes (table I, sheet No. 73). The nonflanged sheet collapsed under a shearing force of  $P_k = 720$  kg; the corresponding displacement amounted to  $\delta = 34 \mu/t$ . With flanged edge of  $D = 52$  the buckling load rose to 1,240 kg, or 72 percent. Admittedly,  $\delta$  likewise rose to  $45 \frac{\mu}{t}$ , that is, 32.5 percent. With still greater holes, but otherwise identical sheets:  $d = 62.2$  (table I, sheet No. 45) which, without flanging, must naturally have still lower buckling values than sheet No. 73, a buckling load of  $P_k = 2,300$  kg was obtained; of course,  $\delta = 130 \frac{\mu}{t}$ , that is, markedly higher. This should be a definite proof of the value of flanging to raise the buckling load in shear. The greater relative displacement  $\delta$  of the flanged versus the unflanged sheet is due to the fact that the flat portion, which after all takes up the greater part of the shearing forces, becomes smaller because of the flanging.

Lastly, we investigated several full sheets (without holes) and compared the obtained buckling load with Southwell and Skan's data (reference 6). The agreement is close according to table I, sheets Nos. 74 to 78. The conclusion that the accord between the theoretical and experimental values for flanged sheets is close, is therefore justified.

In order to determine whether and to what extent a flanged sheet is more resistant to buckling than a smooth, full sheet, we included in table I, aside from  $a_0$  (equation 4) and  $P_{k0}$  (equation 7) the  $P_{ku}$  value of the full sheet (equation 2). It was found that, particularly thin, wide sheets which without holes have a very low buckling load in shear  $P_{ku}$ , the stiffening influence of flanged holes results in a many times greater  $P_{ku}$ ; while in thicker, narrower sheets, inherently very resistant to bending, the higher stress due to reduction in effective, flat surface, it results in weakening. Admittedly, it is necessary to decide in each individual case, whether stiffening or weakening occurs by a comparison of  $P_{k0}$  with  $P_{ku}$ .

REFERENCES

1. Bryan, G. H.: On the Stability of a Plate Under Thrusts in Its Own Plane, with Applications to the "Buckling" of the Sides of a Ship. Proc. of the London Math. Soc., vol. 22, 1891, p. 54.
2. Lilly, W. E.: Web Stresses in Plate Girders and Columns. Engineering, February 1, 1907, pp. 136-139.
3. Lilly, W. E.: The Design of Struts. Engineering, vol. 85, 1908, pp. 37-40.
4. Timoschenko, S.: "Über die Stabilität versteifter Platten; Der Eisenbau, vol. 12, 1921, pp. 147-163.
5. Ritz, W.: "Über eine Methode zur Lösung gewisser Variationsprobleme der mathematischen Physik. Journal f. d. reine und angew. Mathematik, vol. 135, p. 1. (See also his collected works, Paris, 1911.)
6. Southwell, R. V., and Skan, Sylvia W.: On the Stability Under Shearing Forces of a Flat Elastic Strip. Proc. Roy. Soc., series A, vol. 105.
7. Coker, E. G.: Optical Determination of the Variation of Stresses in a Thin Rectangular Plate Subjected to Shear. Proc. Roy. Soc., series A, vol. 86, 1911, pp. 291-319.
8. Bollenrath, Fr.: Ausbeulerscheinungen an ebenen, auf Schub beanspruchten Platten. Luftfahrtforschung, vol. 6, 1930, pp. 1-17.
- ✓ 9. Mathar, J.: Beitrag zur Schubsteifigkeit und Knickfestigkeit von gelochten dünnen Platten. Abhdlg. a. d. Aerodyn. Inst. d. Technical High School, Aachen, No. 10, 1931.
10. Seydel, E.: Beitrag zur Frage des Ausbeulens von versteiften Platten bei Schubbeanspruchung. Luftfahrtforschung, vol. 8, no. 3.
11. Schmieden, C.: Das Ausknicken versteifter Bleche unter Schubbeanspruchung. Z.F.M., vol. 21, 1930, p. 61.

22

N.A.C.A. Technical Memorandum No. 756

12. Bergmann, S., and Reissner, E.: "Über die Knickung von Wellblechstreifen bei Schubbeanspruchung. Z.F.M., Sept. 28, 1929, p. 475; and Z.F.M., vol. 21, 1930.

13. Jennissen, J.: "Über Wellblech bei Schubbeanspruchung. Diss. Aachen, 1931. (Unpublished.)

14. Hirota, M.: "Über den Spannungszustand in einem durchlochten Streifen. Diss. Aachen, 1931.

Translation by J. Vanier,  
National Advisory Committee  
for Aeronautics.

Table 1

Sheet No.	s	a	d	L	P <sub>k</sub> kg	r <sub>k</sub> μ	P <sub>k</sub> kg	λ	μ	Mean- Calcu- lated	Sheet No.	s	a	d	L	P <sub>k</sub> kg	r <sub>k</sub> μ	P <sub>k</sub> kg	λ	μ	Mean- Calcu- lated														
1-6 7-8 9-10 11-12	0,52  0,015  0,8	71 70 82  80 61  76  80 89  76	~ 0,8 D ~ 0,8 D   ~ 0,8 D	~ 1192    ~ 1192    ~ 1192    ~ 1192	1500 1510 1630  1710 1730 1600  2500 1840  1460 1500  1580 2400	295 290 165  131 120 173  107 82  214 171  195 221	0,63 0,633 0,685  0,75 0,73 0,67  1,0 0,77  0,612 0,63  0,693 1,05  0,435 0,473  0,21 0,004 0,608 0,608 0,637 0,592 0,647  0,638 0,592 0,537 0,487 0,555 0,658 0,707 0,922  0,922 0,07 1,02 1,22 1,26  0,508 0,63  0,305 0,368 0,330 0,503 0,668 0,63 0,688 0,676	107 132 95  77 76 108  70 44,5  146 114  124 92  352 230  148 168 171 130  102 111 89 70 60 134 103 85,5  08 141 60,5 64  208 123  237 550 164 184 208 132	0,465 0,318 0,227  0,182 0,175 0,237  0,188 0,166  0,584 0,272  0,293 0,222  0,840 0,648  0,353 0,59 0,568  0,4 0,408 0,332  0,243 0,235 0,205 0,198 0,176 0,136 0,32 0,258 0,207  0,162 0,330 0,237 0,162 0,128  0,505 0,293  0,573 1,31 0,533 0,435 0,457 0,446	0,431 0,307 0,233  0,186 0,252  0,183 0,112  0,353 0,208  0,288 0,21  0,725 0,615  0,312 0,558  0,397 0,397 0,303  0,24 0,24 0,198 0,176 0,136 0,325 0,248 0,196  0,14 0,333 0,237 0,143 0,118  0,634 0,343  0,67 1,32 0,542 0,44 0,42 0,42	44 45   46 47 48 49  50 51  52    54 55 56 57 58 59  60 61 62  63 64 65  66 67 68 69 70  71 72  73 73*)  74 75 76 77 78	0,8    0,8 0,615  0,42 0,52   0,615 0,8  0,52  0,8 0,62  0,55    0,625 0,8  0,165 0,100  0,8 0,125  0,625 0,8  0,625  0,816	56,2 62,25   102 118 76 89  89 97 100    80 97 89  106,5 118  80 97  106,5 118  80 97 118  100,5 107 100,5  80 106,5  80 82  71 76  71 76  71 76 82 89  71 82 80	1690 1690   1690 1690 1430 3210  1690 1010  1600    540 560 580 1290 1900 1600  1300 1180 1170  1400 2580 3700  800 970 1460  1270 1370   1090 720 1240  1192 800  1600 1600  1168 1192 0050	2300 2300   2000 1400 427 374  1500 347  197    325 213 134 630 580 401  217 162 400  382 390 290  376 204 331  300 234  360  360 292  24 50 50  40 65 60  40 55 60 2 137	293 298   170 94 47 374  540 347  197    325 213 134 630 580 401  217 162 400  382 390 290  376 204 331  300 234  360  360 292  24 50 50  40 65 60 2 137	0,68 0,68   0,632 0,413 0,6 1,35  0,63 0,675  0,671    0,227 0,272 0,243 0,642 0,592 0,97  0,645 0,495 0,491  0,687 1,09 1,55  0,336 0,0 0,276 0,608 0,85 0,44 0,633 1,44 0,94  0,302 0,62 0,672  0,597 err. 0,358 err. 0,69 err. 0,722 err. 0,737 err. 0,722 err. 1,01 err. 1,25 err. 2,78 err. 2,61	123 130   88 67 298 116  361 215  123    602 328 231 490 305 251  166 120 393  272 161 78  470 210 228  307 170  518 208  34 46  46,5 36,5 35 28,5 22,5	0,43 0,44   0,304 0,243 0,78 0,785  0,845 0,513  0,398 0,322    1,45 0,78 0,60 1,18 1,09 0,96  0,398 0,312 0,946  0,658 0,56 0,191  1,12 0,502 0,548  0,76 0,41  1,24 0,495  0,115 0,162  0,105 0,079 0,076 0,0623 0,049	0,42 0,42   0,283 0,230 0,785 0,202  0,407 0,305 0,87  0,632 0,354 0,182  1,24 0,470 0,67  0,736 0,414  1,27 0,402  0,128 0,091 0,073 0,073 0,0016 0,0464															
																					D = 62 mm, b = 70 mm														
																					D = 62 mm, b = 90 mm														
																					D = 62 mm, b = 110 mm														
																					D = 82 mm, b = 80 mm														
																					D = 82 mm, b = 110 mm														
																					D = 82 mm, b = 175 mm														
																					D = 82 mm, b = 215 mm														
																					D = 82 mm, b = 110 mm, not flanged														
																					D = 82 mm, b = 110 mm, no holes														

Sheet 73 flanged to D = 52 mm

H.A.C.A. Technical Memorandum No. 755 Table 1





Figure 1.-  
Buckling  
in shear  
on a  
flat  
sheet.

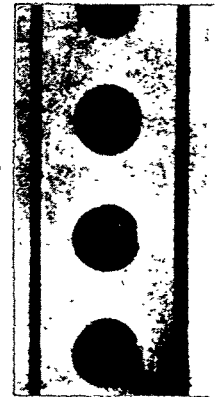


Figure 3.-  
Flanged  
sheet.

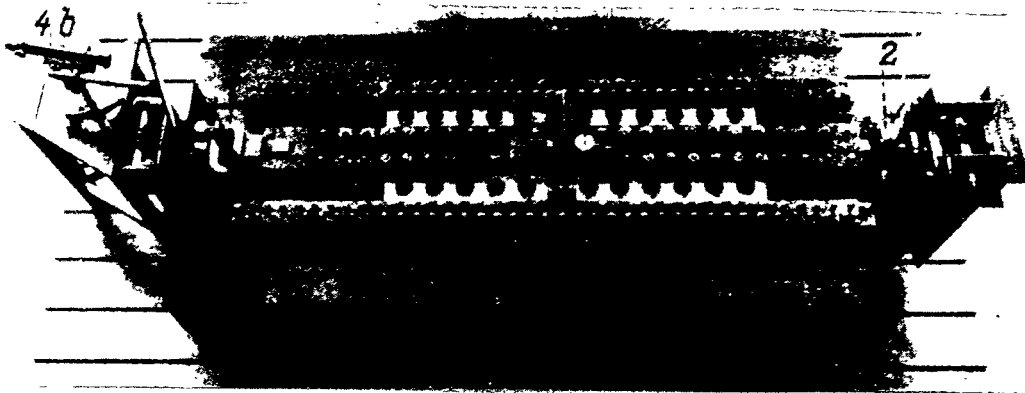


Figure 2.-Experimental setup.

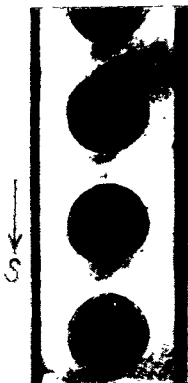


Figure 5.-  
Buckling  
in shear  
on a  
flanged  
sheet.



Figure 9.-  
Sheet  
distorted  
in shear  
showing  
torn  
flanging.

N.A.C.A. Technical Memorandum No. 756

Figs. 4,6

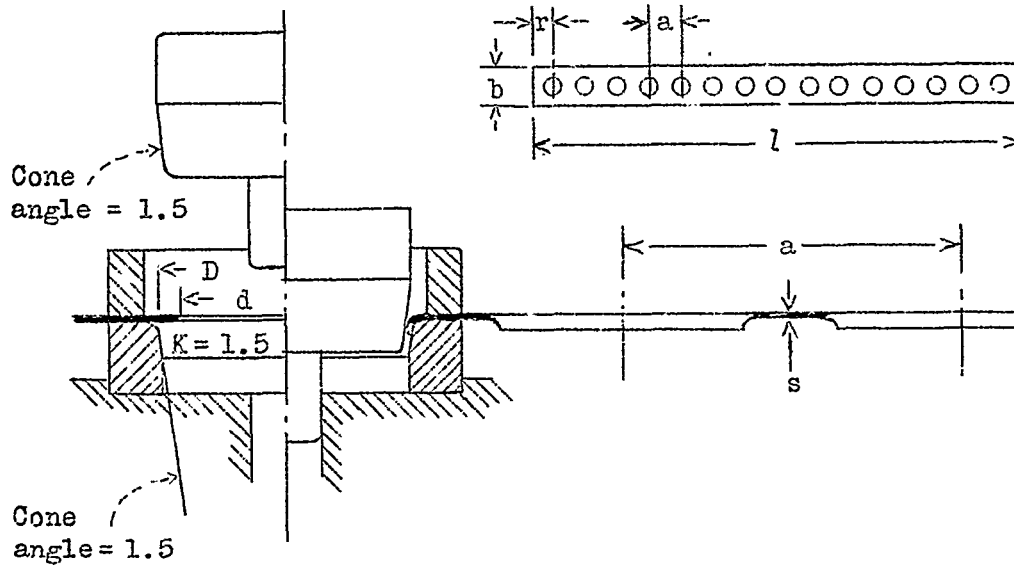


Figure 4.- Flanged sheet and flanging equipment.

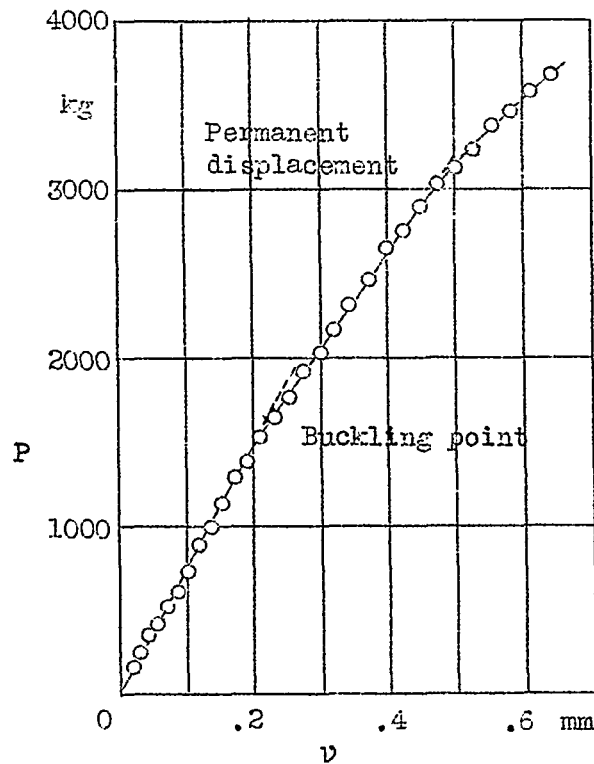


Figure 6.- Shearing force-displacement diagram.

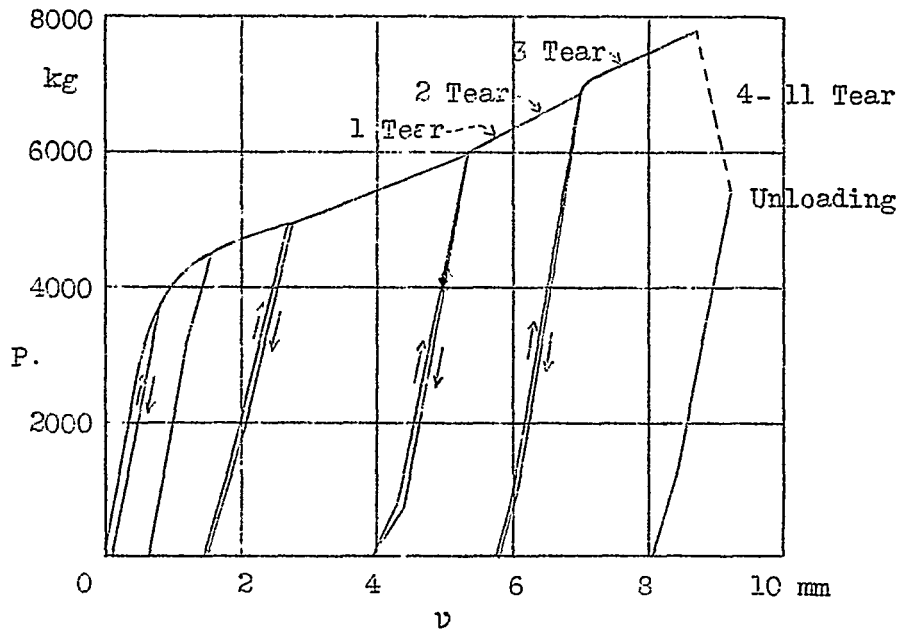


Figure 7.- Shearing force-displacement diagram with great displacements.

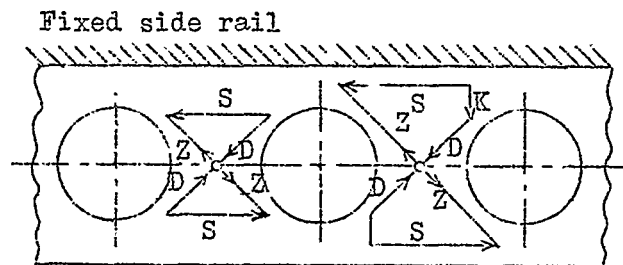
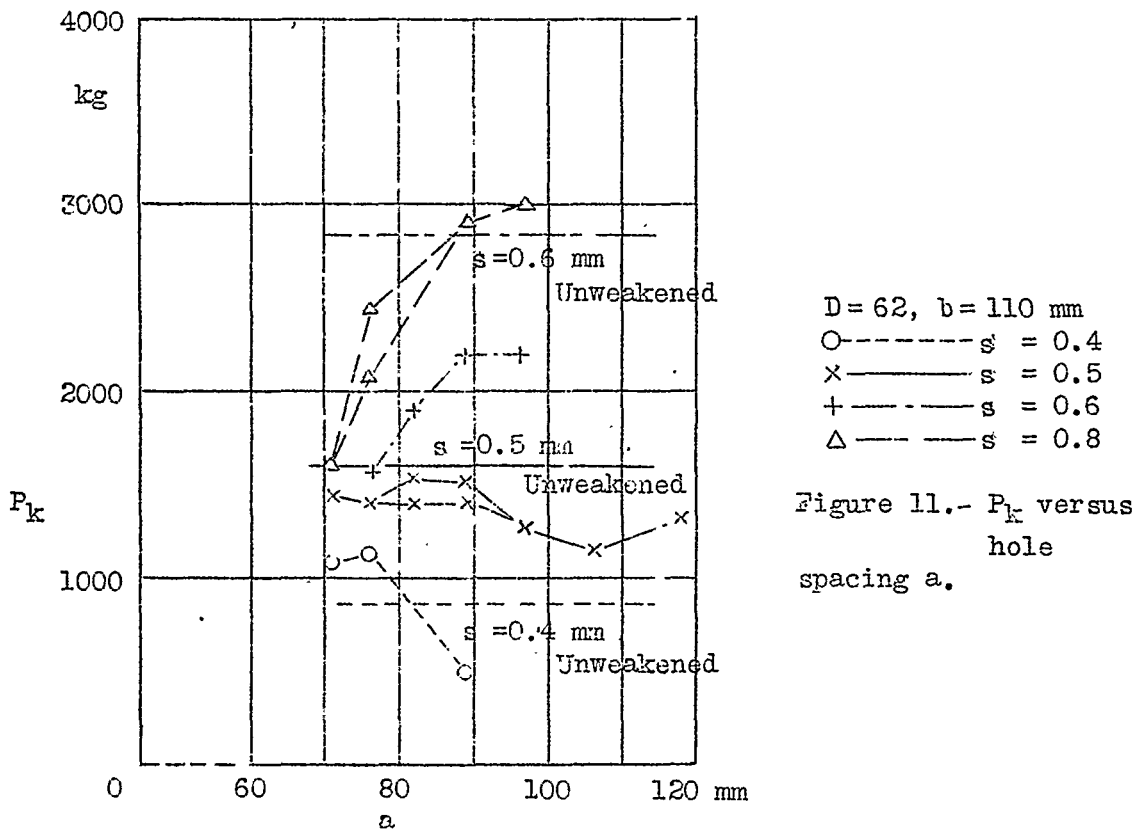
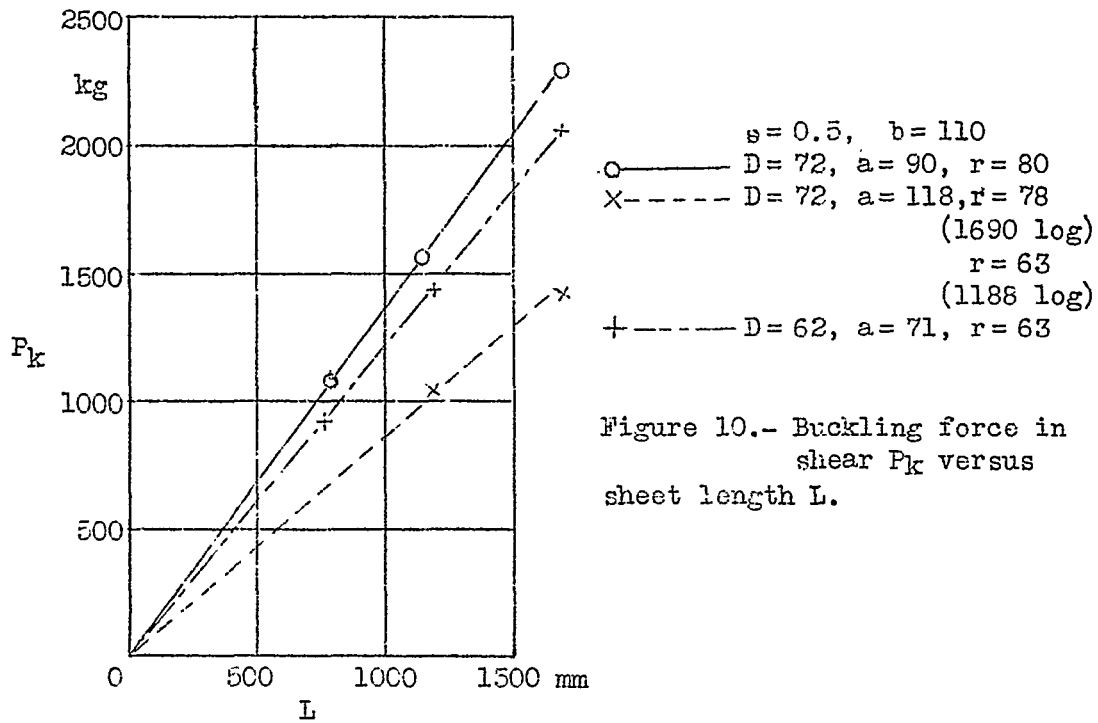


Figure 8.- Distribution of shearing force before and after buckling.



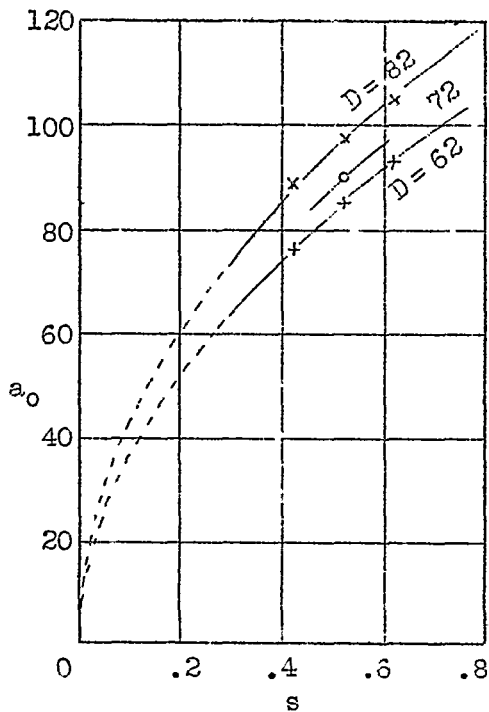


Figure 12.- Optimum hole spacing  $a_0$  versus sheet thickness  $s$ .

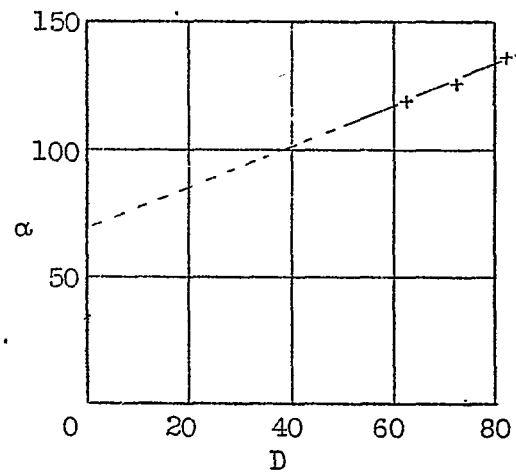


Figure 13.- Factor  $\alpha$  versus D.

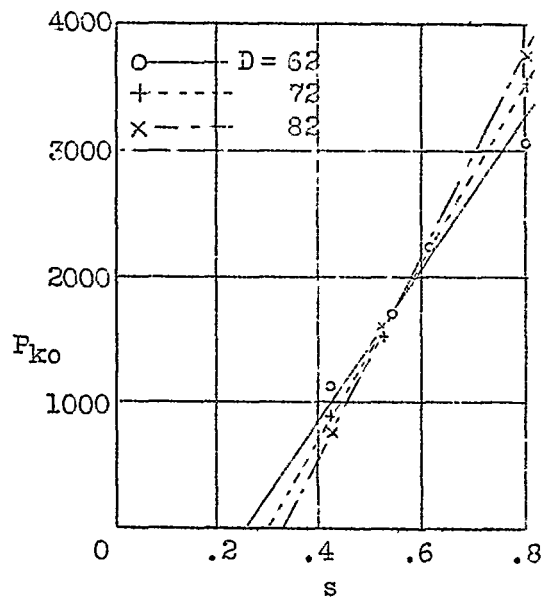


Figure 14.- Optimum  $F_{ko}$  versus  $s$

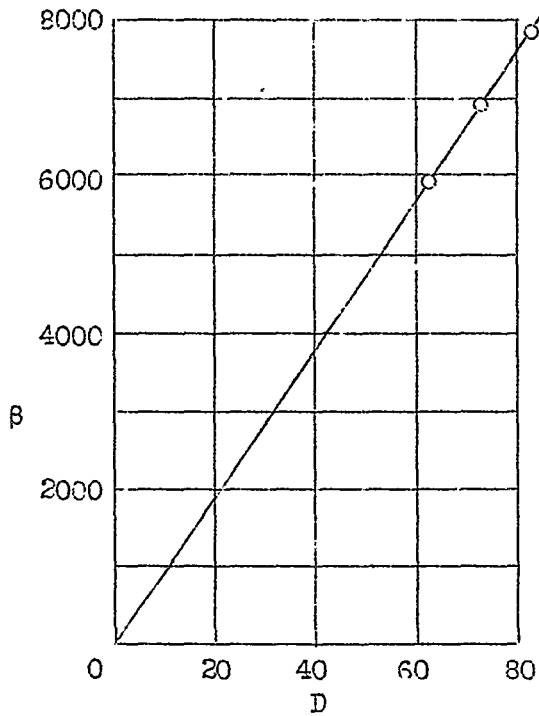


Figure 15.- Factor  $\beta$  versus D

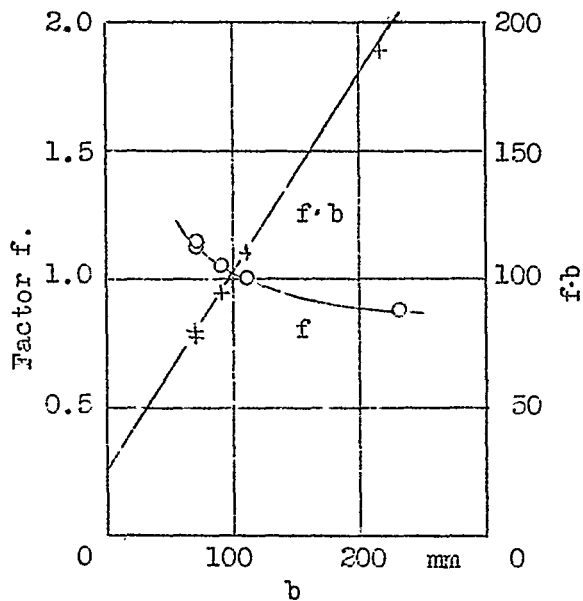


Figure 16.- Correction factor f versus b.

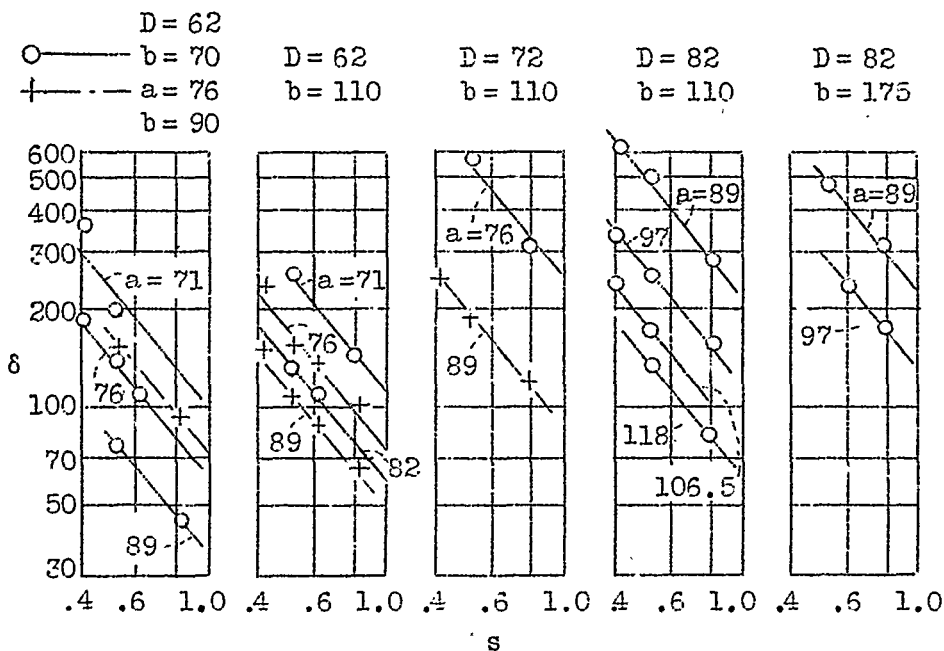


Figure 17.- Displacement  $\delta$  for 1 kg shearing force versus  $s$  (log scale).

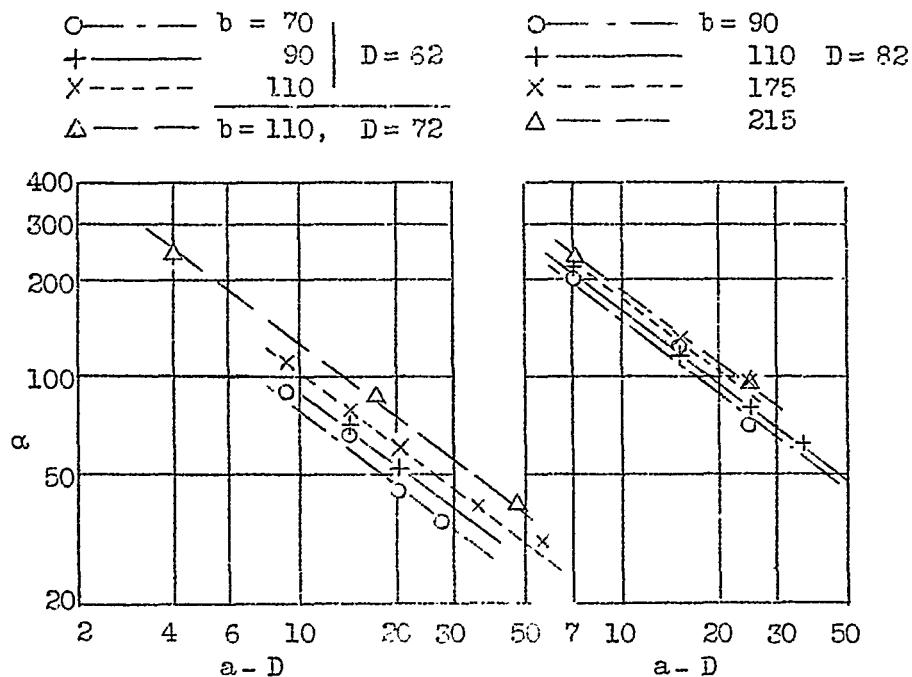


Figure 18.- Coefficient  $\alpha$  versus space ( $a - D$ ) between flangings.

N.A.C.A. Technical Memorandum No. 756

Figs. 19,20

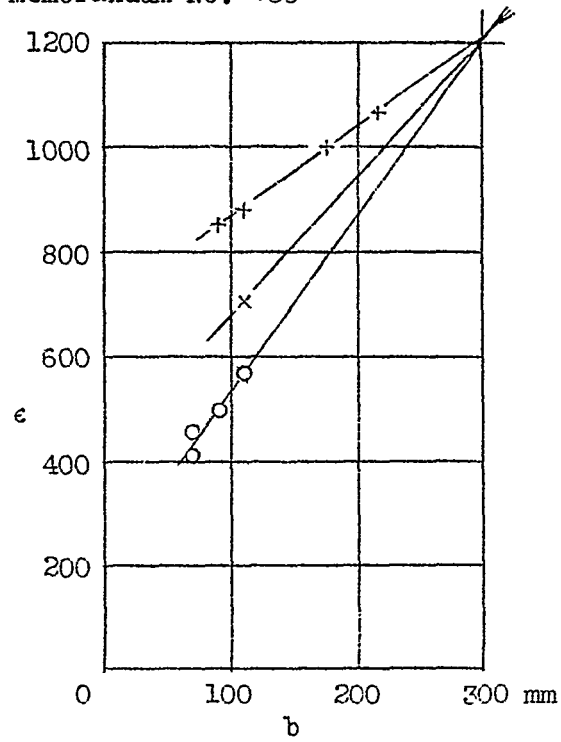


Figure 19.- Factor  $\epsilon$  versus  $b$ .

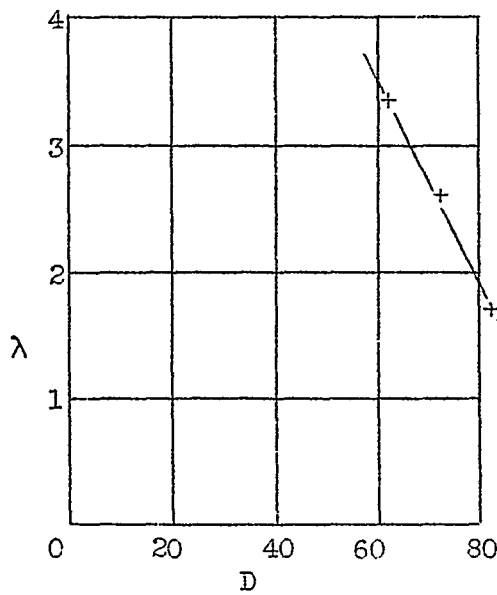


Figure 20.- Slope  $\lambda$  of straight line of figure 19 versus  $D$ .





TECHNICAL LIBRARY

NASA Technical Library

ABBOTT.AEROSPACE.COM



3 1176 01441 1434